Stress and stress relaxation in integrated circuit metals and dielectrics

Bruce L. Draper and Thomas A. Hill
Sandia National Laboratories, Albuquerque, New Mexico 87185

(Received 18 December 1990; accepted 29 April 1991)

In order to provide data needed in the investigation and modeling of stress voiding in integrated circuit metallizations, stress and stress relaxation in Al/Si/Cu alloys and common dielectrics were studied as a function of storage temperature and deposition conditions. It was found that the room-temperature tensile stress in Al/Si/Cu increases with increasing substrate bias and deposition temperature, and that the isothermal relaxation rate upon cooling from 400 °C is sharply dependent on temperature. The activation energy for the relaxation process was found to be 0.39 eV above 130 °C and about 0.08 eV at lower temperatures. For insulating layers deposited with plasma-enhanced chemical-vapor deposition techniques, strong correlations were found among stress, density, hydrogen content, deposition temperature, and film composition (oxides, nitrides, and several intermediate oxynitrides), with the highest levels of compressive stress (near 1 GPa) being measured in nitride films deposited at 300 °C. These films, as well as phosphorus-doped glasses used as capping/protection layers, were found to undergo structural changes upon post-deposition thermal cycling which affected stress levels.

I. INTRODUCTION

Because of its catastrophic effects, stress voiding in integrated circuit (IC) metallization layers has garnered much recent attention.[1-4] ICs suffering from this malady perform normally immediately after fabrication, but are found to be nonfunctional after unpowered storage for an extended period (months to years). Failure analysis shows that the metal wiring lines, which are most often 1 to 5 μm wide and about 1 μm thick, contain large numbers of voids – some of which span the entire width of a line and create an "open" circuit (see Fig. 1, for example). This is a serious problem for all IC manufacturers and users, but is even more critical for those in the weapon and deep-space probe communities who require microelectronics functionality after long-term storage.

While much effort has gone into finding ways to accelerate stress voiding so that an existing IC's susceptibility to failure can be determined, comparatively little is known about the basic physical mechanisms. Several theoretical models of the voiding process have been published recently,[5-8] but all rely on a multitude of material properties—many of which are poorly known. In addition, a great deal of information is needed in aid of finite-element modeling of stresses in the complete substrate/metal/dielectric system. It is the intent of the work described here to provide much of the stress and stress relaxation data needed to support the modeling efforts. To begin the study, stresses in aluminum–silicon–copper alloys were examined as a function of temperature and deposition conditions. In normal processing, the aluminum-based IC metallization layers are deposited at temperatures between 100 and 350 °C but are subsequently exposed to multiple thermal cycling from room temperature to 450 °C (for dielectric depositions, annealing, and packaging operations). Therefore, it is important to characterize metal film stress over a very wide temperature range. In addition, the time dependence (relaxation) of metal stress was examined as a function of storage temperature (25–180 °C).

A complete understanding of voiding processes in aluminum IC metallizations requires knowledge of not only the stress inherent in the basic metal layers but also the stresses induced by intermetal and capping dielectrics. Typically, these insulating layers are deposited at temperatures between 250 and 400 °C by plasma-enhanced, low pressure, or atmospheric pressure chemical vapor deposition (CVD), and may undergo further processing at temperatures up to 450 °C (e.g., for metal/semiconductor or metal/metal contact alloying). Some authors have reported that the density and size of metal voids are dependent on the dielectric film stress,[3-5] while others suggest that additional properties such as density and hydrogen content may also effect void formation.[3,9-11] Consequently, it is important to characterize in this study the dependence of many dielectric film properties on deposition/postprocessing conditions.

II. EXPERIMENTAL PROCEDURE

All samples used in this study were prepared and tested in Sandia National Laboratories' Microelectronics Development Laboratory, a Class 1 clean room facility currently supporting a large number of technologies. High quality, 150-mm diameter, *n*-type silicon substrates of (100) orientation and 675 μm nominal thickness were prepared for the experiments by cleaning in a sulfuric acid/hydrogen peroxide solution, followed by a 15:1 H_2O:HF etch and deionized water rinse. The wafers to be used in metallization experiments were first oxidized at 1050 °C in steam. Metal (Al/1%Si or Al/0.75%Si/0.5%Cu) was then deposited in an automated, load-locked dc magnetron sputtering system with a base pressure below 10^{-6} Pa. Substrate temperature at the time of metal deposition was varied from 30 to 250 °C.

Plasma-enhanced CVD (PECVD) oxide, oxynitride, and nitride films typical of those used as insulating layers between metal levels in ICs were deposited in an automated, load-locked, parallel-plate, rf plasma reactor. In this system, batches of wafers were loaded onto a grounded electrode which rotated at 2 rpm during deposition. The upper electrode (which also contained heating elements) was powered with a 6 kW, 380 kHz rf supply. Reactant gases (SiH_4, N_2O,

 0734-211X/91/041956-07$01.00

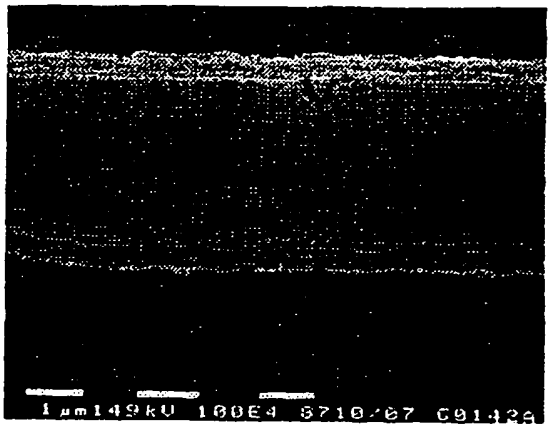

FIG. 1. SEM of an open-circuit condition created by stress voiding in an IC metallization line.

N_2O, NH_3, and N_2) were premixed and injected from a single nozzle near the perimeter of the electrodes. Film composition was varied by adjusting the ratios of N_2O to SiH_4 and $NH_3 + N_2$ to SiH_4 (see Table I) while holding the total flow constant at 1760 sccm. The pressure, rf current density, and SiH_4 flow were maintained at 43 Pa, 292 $\mu A/cm^2$, and 110 sccm, respectively. Deposition temperature was held at 300 °C except for the various "midpoint" oxynitrides (described later) which were deposited at 250, 300, and 350 °C.

The phosphorus-doped glasses studied here and often used as IC capping layers were deposited by both atmospheric and low-pressure CVD (APCVD and LPCVD) techniques using SiH_4, PH_3, and O_2 source gases. A belt-driven atmospheric-pressure batch reactor was utilized to deposit 5 wt. % phosphorus-doped glass at 420 °C and at a rate of about 50 nm/min. A more modern single-wafer LPCVD (80 Pa) reactor was used to deposit 3 wt. % P-glass at 350 °C at a rate of approximately 20 nm/min.

Thin-film stress (in the metal and dielectric layers) was calculated from wafer curvature measurements made with a laser-based instrument manufactured by FLEXUS, Inc. Metal stress measurements made in this rapid, straightforward manner were previously found to agree with those from more elaborate x-ray diffraction studies of the same samples.[12] The FLEXUS instrument also contains a heated wafer chuck (25–450 °C) which facilitated the study of thin-film stress over the temperature range normally encountered in IC processing after metal deposition. For measurements of dielectric film stress, film thicknesses between 450 and 600 nm were chosen based on the refractive index to avoid destructive interference effects at the measurement wavelength (633 nm).

Dielectric film thickness and refractive index were measured using an automated ellipsometer operating at a wavelength of 633 nm. For each film type, initial depositions were made with film thicknesses near the center of the first ellipsometric order (approximately 100 nm) for accurate calculation of the refractive index. The refractive index was subsequently fixed for the measurement of thicker films used for stress measurements.

Dielectric film density was calculated from the measured weight of the film, average film thickness, and the area of the substrate (which was calculated from the weight of the bare wafer, average thickness of the wafer as determined by differential capacitance measurements, and an assumed silicon density of 2.328 gm/cm^3). Measurements were averaged over three samples for each film type.

Hydrogen content of the films was measured using 24 MeV Si elastic recoil detection (ERD).[13] The Si beam was incident on the sample at an angle of 75° degrees, and recoiled hydrogen ions were detected at a forward scattering angle of 30° degrees after passing through a Mylar range foil. Using this method, the detection limit for hydrogen is approximately 0.1 at. % and the depth resolution is about 50 nm.

TABLE I. Deposition conditions for PECVD films.

Film	Gas flows (sccm) SiH_4	N_2O	NH_3	N_2	Temperature (°C)
Oxide	110	1760	0	0	300
Oxy-1	110	1320	220	220	300
Oxy-2[a]	110	880	440	440	250, 300, 350
Oxy-3	110	440	660	660	300
Nitride	110	0	880	880	300

[a] "Midpoint" oxynitride.

III. EXPERIMENTAL RESULTS AND DISCUSSION

Figure 2 shows a plot of stress versus temperature for a 1 μm Al/Si/Cu film deposited at 150 °C on oxidized silicon. Plots such as this have appeared in numerous publications[14,15] and are all remarkable in their similarities, despite

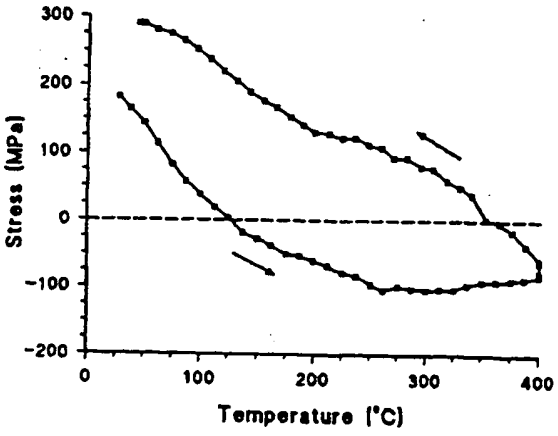

FIG. 2. Stress vs temperature for a 1 μm thick Al/Si/Cu film deposited at 150 °C. As is the case for all figures, positive values represent tensile stress while negative values correspond to compressive stress.

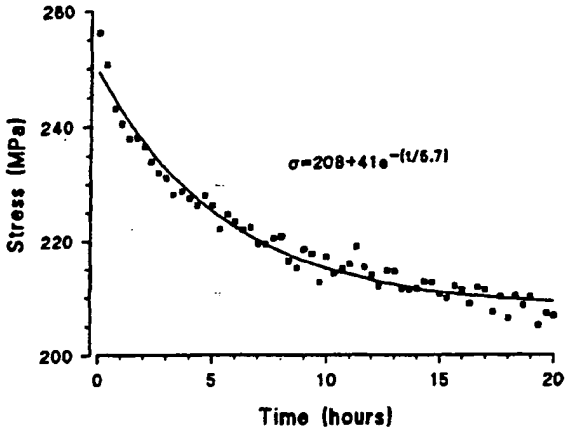

FIG. 3. Stress vs time for an Al/Si/Cu film held at 70 °C (after cooling from 400 °C).

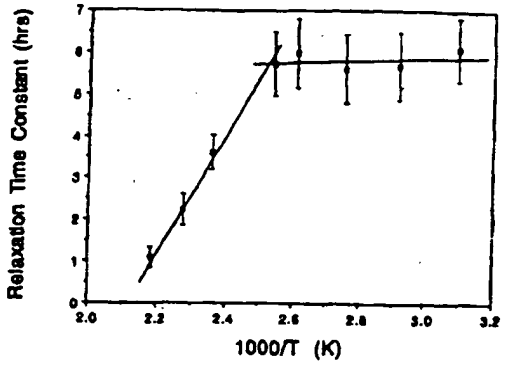

FIG. 5. Relaxation time constant vs relaxation temperature for 1 μm thick Al/Si/Cu films deposited at 150 °C.

differences in deposition conditions and alloy content (pure Al, Al/Si, and Al/Si/Cu of various concentrations and even Al/Si/Ti when the Ti content is not excessive). The metal stress, resulting from differences in thermal expansion coefficients between Al and Si, is tensile at room temperature but decreases as the temperature is increased and the film expands elastically. Above about 200 °C plastic deformation occurs and the stress remains low. As it cools, the film again contracts more quickly than the silicon substrate and large tensile stresses are generated (the upper portion of Fig. 2). If the temperature cycle is paused during the cool down, it is possible to watch the stress relax with time. Figure 3 shows a plot of stress σ generated in this way at 70 °C. Also plotted in Fig. 3 is an equation of the form

$$\sigma = A + Be^{-t/\tau},$$

where t is time and A, B, and τ are constants. While the physical mechanisms responsible for stress relaxation in aluminum thin films may best be described by some other function, the fit to an exponential is exceptionally good and the calculation of τ, the relaxation time constant, is very useful in comparing the relaxation rates of various films. This information on global stress relaxation is needed in the stress voiding models.

The stress relaxation time constant for Al/Si/Cu at 70 °C is shown versus metal grain size in Fig. 4 [average metal grain size was determined from scanning electron micrographs (SEM) of decorated samples]. It can be seen in this plot that τ is proportional to the grain size. Stress relaxation in Al alloy thin films occurs by mass transport, and the easiest path for transport is through grain boundaries. Films with larger grains have fewer grain boundaries and, therefore, less mass transport along boundaries can take place.

Figure 5 shows the relaxation time constant versus relaxation temperature for 1 μm Al/Si/Cu films deposited at 150 °C. Note that there are clearly at least two independent mechanisms involved in stress relaxation, one dominant at temperatures above 130 °C and the other operable below 130 °C (and very nearly independent of temperature). If the initial rate of relaxation is plotted versus temperature (Fig. 6), the activation energies for the two processes can easily be

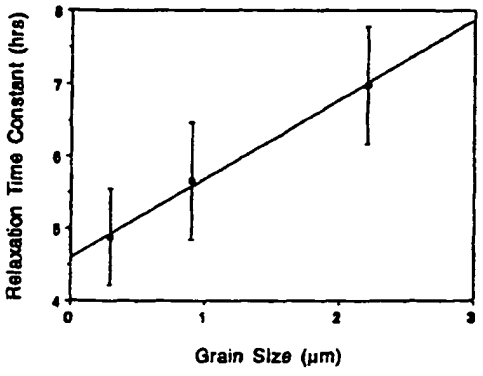

FIG. 4. Stress relaxation time constant at 70 °C vs metal grain size for Al/Si/Cu films.

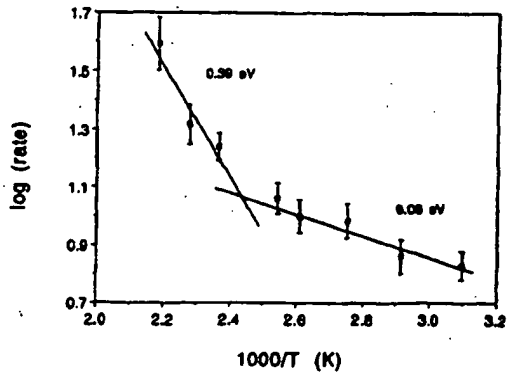

FIG. 6. Initial relaxation rate vs temperature for Al/Si/Cu films deposited at 150 °C.

calculated. The first, 0.39 eV, is consistent with mass transport through grain boundary diffusion. (The activation energy for the time constant alone in this temperature regime is 0.57 eV). The activation energy for the low-temperature stress relaxation rate in Al/Si/Cu appears to be very much lower and may be representative of surface diffusion mechanisms. A previous study using pure aluminum deposited through electron-beam evaporation yielded an activation energy for tensile stress relaxation of 0.23 eV between the temperatures of 220 and 87 °C.[16]

A contour plot of Al/Si/Cu stress at room temperature as a function of deposition conditions (substrate temperature, rf substrate bias, and sputtering cathode power) is displayed in Fig. 7. For the sputtering apparatus used in this study, films of low tensile stress (and less prone to stress voiding, according to theory) can be produced by not heating the wafers during deposition and by not using substrate bias. Unfortunately, other IC technology constraints (e.g., electromigration resistance and film conformality) require elevated deposition temperatures and/or bias. Understanding the effects of deposition parameters on stress will allow optimization of film performance with respect to all constraints.

Several properties of PECVD dielectric films that may be correlated to stress were measured for film compositions ranging from oxide to nitride. In addition, stress was measured as a function of deposition temperature for the midpoint oxynitride (one which, in terms of gas composition, is midway between oxide and nitride; see Table I). Figure 8 shows the refractive index, density, etch rate in 100:1 H_2O:HF, hydrogen concentration, and room-temperature stress as a function of composition for depositions at 300 °C. The relationship between refractive index and film density is well known from the Lorentz–Lorenz relationship. Also evident in Fig. 8 is the fact that stress and hydrogen concentration also have strong correlations to refractive index and density. Figure 8(a) compares the stress of dielectric films deposited on bare silicon and on Al/Si/Cu. Here, the dielectric film stress on metal is 10% to 30% lower than on silicon (except for oxide films, where the stresses appear to be independent of the underlying material). The difference may be due to interfacial effects: the metal may act as a "buffer" layer, relieving some of the dielectric stress. Further evidence of this behavior is noted in the observation that the stress of PECVD films deposited on oxidized silicon was identical to that of films deposited on bare silicon. The anomalous etch rate behavior seen in Fig. 8(c) is uncorrelated to the other dependent variables studied here and may be due to the relative concentration and bond strengths of SiH and NH in the films. The actual concentration of SiH and NH in these films is currently being investigated.

Figure 9 shows similar data as a function of deposition temperature for the midpoint oxynitride. In this case, there is a strong correlation between refractive index, density, etch rate, hydrogen concentration, and stress. It should be noted that ERD measurements of hydrogen concentration were performed on films deposited on both bare silicon [Figs. 8(b) and 9(b)] and on Al/Si/Cu. Interestingly, the measurements of films deposited on Al/Si/Cu indicated that the

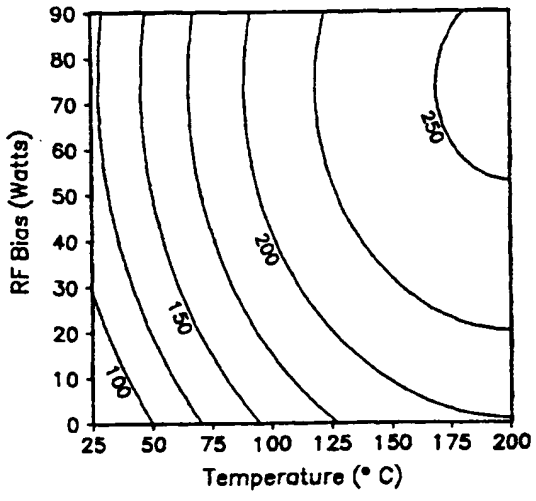

FIG. 7. Contour plot of room-temperature stress (in MPa) in Al/Si/Cu films as a function of substrate bias and temperature during deposition.

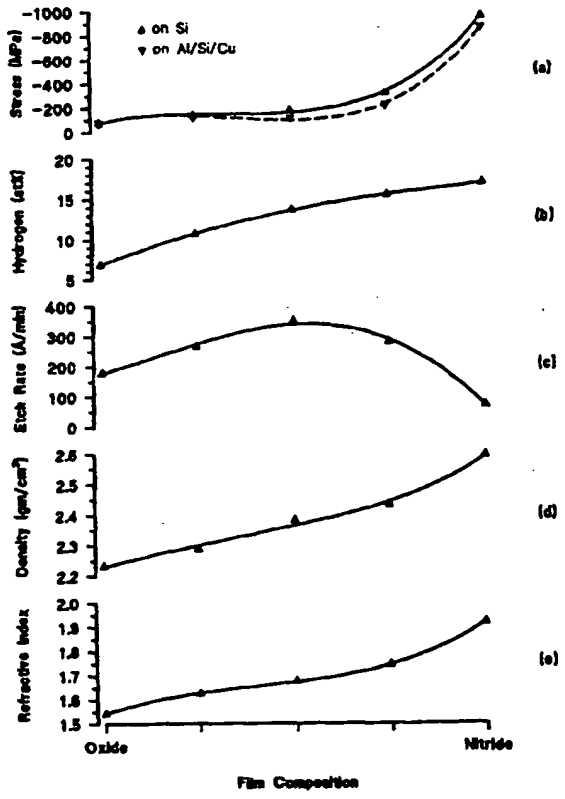

FIG. 8. Room-temperature stress, hydrogen concentration, etch rate in 100:1 H_2O:HF, film density, and refractive index vs film composition. Depositions were done at 300 °C.

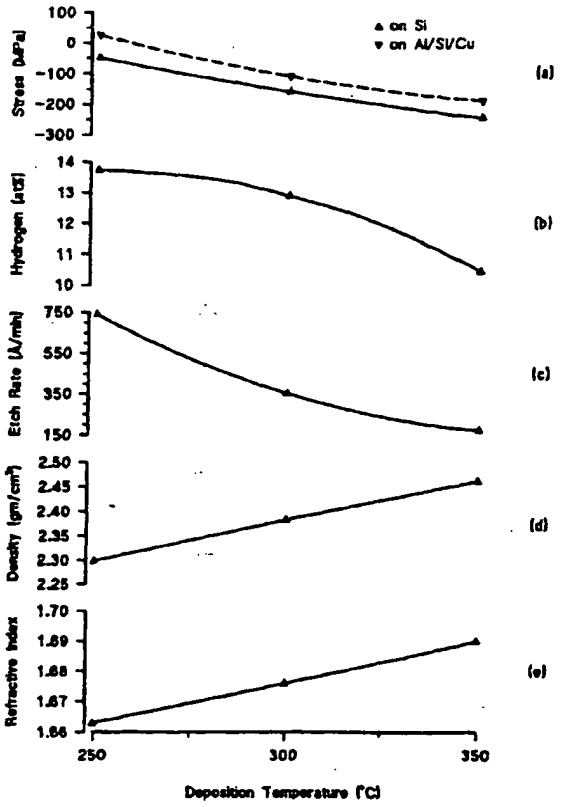

FIG. 9. Room-temperature stress, hydrogen concentration, etch rate in 100:1 H_2O:HF, film density, and refractive index vs deposition temperature for the "midpoint" oxynitride.

hydrogen content was nearly independent of deposition temperature—approximately 13 at. %. Furthermore, the hydrogen content as a function of film composition was consistently higher on Al/Si/Cu than on silicon (except for the plasma oxide once again, which contained 6.3 at. % in both cases). The reason for this difference is not yet clear, but ensuing studies are examining the possible interactions of hydrogen with the metal. Figure 9(a) also compares film stress for depositions on silicon and Al/Si/Cu. As in Fig. 8(a), the observed trend here is for lower stress in films deposited on metal—again suggesting a possible buffer layer effect.

The effect of post-deposition thermal cycling on dielectric stress was studied using the Flexus gauge. Thermal cycles were performed in air by ramping the films from room temperature to 450 °C at a rate of 3 °C/min, soaking at 450 °C for 1 h, slowly cooling to room temperature over a period of several hours, and then repeating the sequence. Figure 10 compares the results for PECVD oxide, oxynitride ($n = 1.68$), and nitride deposited on silicon at 300 °C. In each case, the film stress after thermal cycling is lower, but remains compressive. This behavior suggests a structural change in the films that is probably due to volume contraction (densification). This theory is supported in Fig. 11

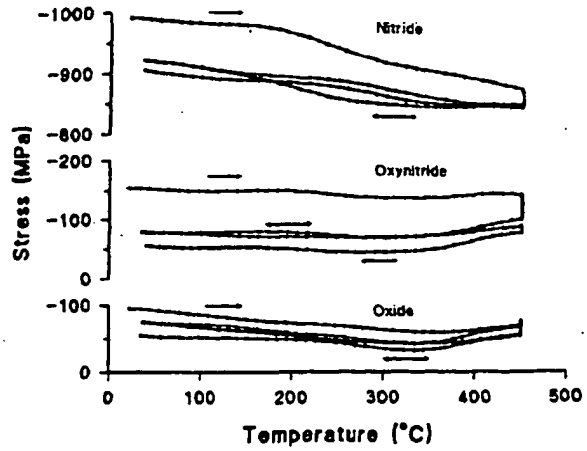

FIG. 10. Stress vs temperature for PECVD oxide, oxynitride, and nitride deposited at 300 °C.

which shows stress versus temperature curves for the oxynitride as a function of deposition temperature. Here, the change toward tensile stress due to thermal cycling is shown to increase with decreasing deposition temperature (i.e., lower as-deposited film density). The measured thickness loss for all films in Figs. 10 and 11 ranged from 0.5 to 2 nm (with no observable change in refractive index), but was not well correlated to the magnitude of the stress change or the as-deposited film density. Therefore, some other structural transformations—including second order effects related to the hydrogen content or bonding—are being investigated.

Figures 12 and 13 show stress versus temperature data for phosphorus-doped glasses deposited on silicon by LPCVD and APCVD. Again, the shape of the curves probably results primarily from densification, although other structural changes such as conversion of phosphorus suboxides also may play a role. Additionally, in contrast to the undoped PECVD films in this study, as-deposited P-glass is hygrosco-

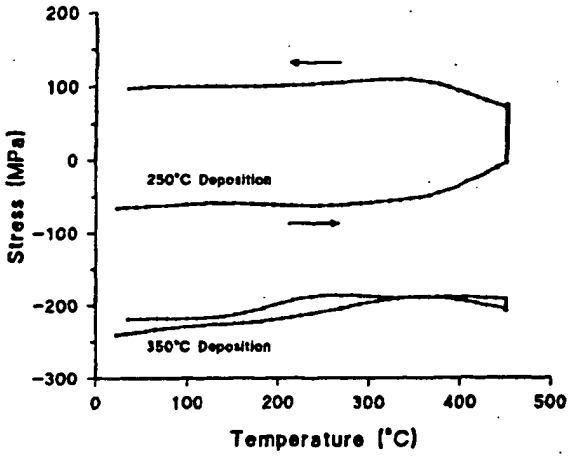

FIG. 11. Stress vs temperature for PECVD oxynitrides deposited at 250 and 350 °C.

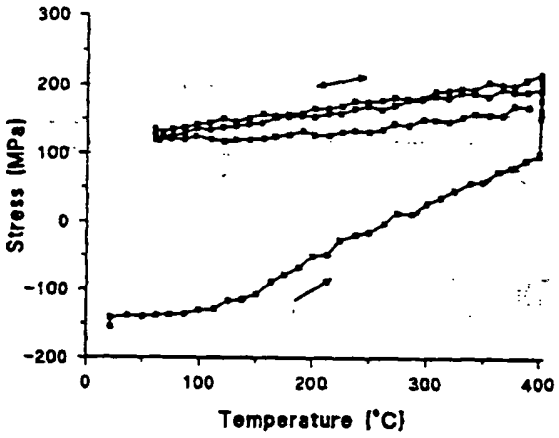

FIG. 12. Stress vs temperature for P-glass deposited by LPCVD.

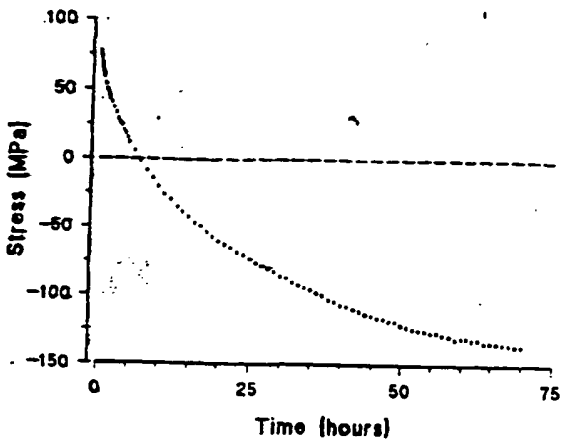

FIG. 14. Stress vs time after deposition for LPCVD P-glass.

pic, a fact which may account for the changes in stress after deposition which were noted in this film (Fig. 14). Similar observations of this effect in P-glass have been reported previously.[17]

Finally, the stress versus temperature behavior of the combined films of PECVD oxynitride deposited on Al/Si/Cu is shown in Fig. 15. The curve has the appearance of a simple superposition of the metal and oxynitride films discussed earlier, leading to the conclusion that no significant interactions occur between metal and PECVD oxynitrides: the curve retains the dominant, hysteretic shape from the Al/Si/Cu, but is displaced by the difference in the room-temperature stresses of the metal and oxynitride. A second thermal cycle shifts the curve further toward tensile stress, again probably due to structural changes in the oxynitride. Similar trends have been noted previously for plasma nitride deposited on aluminum.[18]

IV. SUMMARY

Stress and stress relaxation in Al/Si/Cu alloys were studied as a function of temperature and deposition conditions. Increasing substrate bias and temperature during deposition were found to increase the room-temperature, postdeposition tensile stress in these films. Cycling the metal films between room temperature and 400 °C, as would be done during "normal" integrated circuit processing, produced stress levels varying from slightly compressive to moderately tensile. The isothermal stress relaxation rate which was measured when the films were cooled from 400 °C was found to be dependent on temperature, with activation energies of 0.39 eV and 0.08 eV above and below 130 °C, respectively.

Insulating layers deposited with plasma-enhanced chemical vapor techniques were found to display strong correlations among stress, density, hydrogen content, deposition temperature, and film composition (oxides, nitrides, and

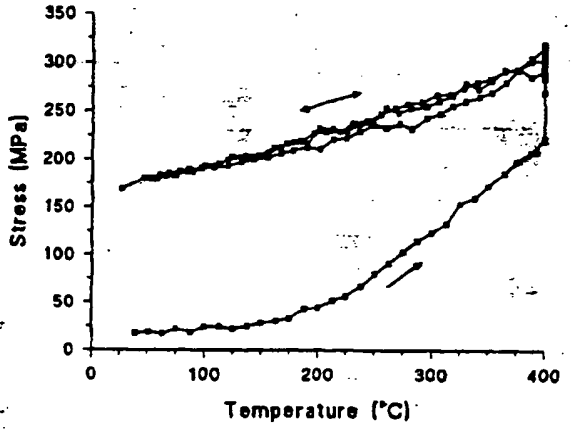

FIG. 13. Stress vs temperature for P-glass deposited by APCVD.

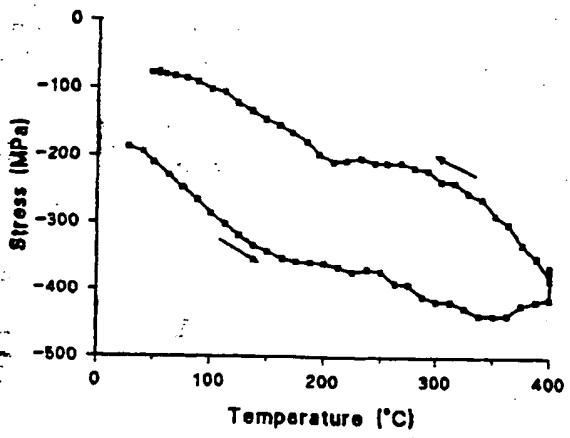

FIG. 15. Stress vs temperature for PECVD oxynitride on Al/Si/Cu.

several intermediate oxynitrides were studied). Compressive stresses—believed to be the most dangerous in terms of their ability to aggravate metal stress voiding—as high as 1 GPa were measured in PECVD nitride films deposited at 300 °C. These films, as well as phosphorus-doped glasses typically used as protection layers on integrated circuits were found to undergo structural and stress changes when thermally cycled.

Based on these results, there are several general conclusions that can be drawn even without the aid of detailed models. First, in order to reduce internal stresses, thermal cycling of metal films should be minimized. Any excursions above about 200 °C produce plastic deformation and higher tensile stresses upon cooling. Of course, lower metal deposition temperatures also lead to reduced stress, but may not be consistent with other requirements such as grain size and step coverage. Insulating layers deposited over metal films should be of low stress. In this study, either simple P-glass films or PECVD oxides and oxynitrides deposited at low temperatures would meet this requirement. As with the case for metal films, thermal cycling of dielectrics should be minimized.

Conversely, researchers interested in accelerating the stress voiding process should use PECVD nitride capping layers over the patterned metal films. In addition, heating the samples to 400 °C and then cooling to about 70 °C (instead of room temperature) not only creates increased tensile stress in the metal films but, because of the elevated temperature, provides a thermal acceleration factor.

ACKNOWLEDGMENTS

The authors gratefully acknowledge the assistance of Glenn Bailey in metal and PECVD operations, Gordon Iben and Manny Gonzales in supplying P-glass samples, and Charles Barbour for ERD analysis. This work performed at Sandia National Laboratories was supported by the U.S. Department of Energy under Contract No. DE-AC04-76DP00789.

[1] J. G. Ryan, J. B. Riendeau, S. E. Shore, G. J. Slusser, D. C. Beyar, D. P. Bouldin, and T. D. Sullivan, J. Vac. Sci. Technol. A 8, 1474 (1990).
[2] W. Tice and G. Slusser, J. Vac. Sci. Technol. B 8, 106 (1990).
[3] J. Curry, G. Fitzgibbon, Y. Guan, R. Muollo, G. Nelson, and A. Thomas, *Proceedings of the 1984 International Reliability Physics Symposium* (IEEE, New York, 1984), p. 6.
[4] K. Hinode, N. Owada, T. Nishida, and K. Mukai, J. Vac. Sci. Technol. B 5, 518 (1987).
[5] J. W. McPherson and C. F. Dunn, J. Vac. Sci. Technol. B 5, 1321 (1987).
[6] F. G. Yost, Scr. Metall. 23, 1323 (1989).
[7] T. Turner and K. Wendel, *Proceedings of the 1985 International Reliability Physics Symposium* (IEEE, New York, 1985), p 142.
[8] Che-Yu Li, Ronald Black, and William R. LaFontaine, Appl. Phys. Lett. 53, 31 (1988).
[9] R. Abermann, Thin Solid Films 188, 385 (1990).
[10] J. T. Yue, W. P. Funsten, and R. V. Tayor, *Proceedings of the 1985 International Reliability Physics Symposium* (IEEE, New York, 1985), p. 126.
[11] A. S. Harrus and E. P. van de Ven, Semicond. Int. 13, 124 (1990).
[12] Lynn E. Lowry, James A. Van Den Avyle, and Bruce L. Draper, presented at the 38th Annual Denver X-ray Conference, July 1989.
[13] B. L. Doyle and P. S. Peercy, in *Proceedings of BES/DOE Workshop on the Analysis of Hydrogen in Solids*, edited by R. L. Schwoebel and J. L. Warren, DOE/ER-0026 (US Department of Energy, Washington, DC, 1979) p. 92.
[14] Donald S. Gardner, Timothy L. Michalka, Paul A. Flinn, Troy W. Barbee, Krishna C. Saraswat, and James D. Meindl, *Proceedings of the Second IEEE VLSI Multilevel Interconnection Conference* (IEEE, New York, 1985), p. 102.
[15] A. K. Sinha and T. T. Sheng, Thin Solid Films 48 (1978), p. 117.
[16] M. Hershkovitz, I. A. Blech, and Y. Komen, Thin Solid Films, 130, 87 (1985).
[17] C. Ramiller and L. Yan, Technical Program Proceedings of SEMICON/West (1982), p. 29.
[18] A. K. Sinha, H. J. Levinstein, and T. E. Smith, J. Appl. Phys. 49, 2423 (1978).